Changes in Magnetospheric Configuration during the Substorm Growth Phase

F. V. CORONITI AND C. F. KENNEL[1]

Plasma Physics Group, Department of Physics
University of California, Los Angeles, California 90024

Three calculations suggest that the magnetospheric configuration changes during the substorm growth phase. A flaring-tail model indicates that the observed increases in geomagnetic tail field are explained if the dayside magnetopause shrinks by 1–2 R_E. Increased tail flaring also requires that the tail current sheet approach near the earth during the growth phase. The motion of the inner edge of the plasma sheet, and consequently an equatorward shift of the nightside auroral oval, is consistent with the structural modifications mentioned above.

In this paper we investigate various changes in the configuration of the geomagnetic tail that occur during the growth phase of magnetospheric substorms. The growth phase commences with a southward shift of the solar-wind magnetic field followed by an inward motion of the dayside magnetopause [*Meng*, 1970; *Aubry et al.*, 1970; *Fairfield*, 1971; *Akasofu*, 1972]. *Aubry et al.* [1970] demonstrated that during nose radius decrease the tail-field strength increased, this increase thus indicating a net flux transport from the dayside magnetosphere into the tail [also see *Fairfield and Ness*, 1970; *Russell et al.*, 1971]. The over-all shrinkage of the dayside magnetosphere's aerodynamic shape suggests that the near-earth tail magnetopause also contracts. Both experiment [*Hones*, 1970] and theory [*Spreiter and Alksne*, 1969; *Tverskoy*, 1968] indicate that the near-earth tail magnetopause must flare to intercept solar-wind dynamic pressure so that the tail is in hydromagnetic-pressure balance. The tail-flux addition and nose shrinkage imply that tail flaring, and thus tail-field strength, should increase during substorm growth phase. In a flaring tail the solar wind exerts a net force on the tail in the antisolar direction. According to *Siscoe and Cummings* [1969], as this force increases, the tail current system must move earthward, its movement thus producing field depressions at the geostationary orbit. Finally, the earthward motion of the tail-like region implies that the inner edge of the electron plasma sheet should also approach the earth during the growth phase. Consequently, the nightside auroral oval should migrate equatorward. Since the above configurational changes follow from enhanced dayside field cutting and magnetopause shrinkage, it seems likely that any change in the internal convection rate triggered by reconnection will be accompanied by changes in the shape of the magnetosphere.

In the next section we review a flaring-tail model originally proposed by *Tverskoy* [1968] and *Spreiter and Alksne* [1969] and shown by Spreiter and Alksne to be in reasonable agreement with magnetic-field observations in the geomagnetic tail [*Mihalov et al.*, 1968; *Behannon*, 1968, 1970]. For constant solar-wind conditions this model is parametrized by three quantities, variations of which we estimate to calculate tail-field changes during growth phase: the flux in the tail, the distance downstream where the tail solution first applies, and the initial radius of the tail at that distance. The changes in tail flux and initial tail radius can be estimated from the dayside magnetopause motions; however, the variation of the downstream distance to the inner edge of the tail current system is not specified. To estimate this parametric change, we modify, to suit a flaring tail, the method of estimating the downstream distance to the taillike region proposed by *Siscoe and Cummings* [1969]. Whereas they assumed that the tail radius would increase if the tail flux increased, a nonflaring-tail assumption, observation indicates the tail radius should de-

[1] Alfred P. Sloan Foundation Faculty Fellow.

crease simultaneously with tail-flux increases. This effect would enhance the inward motion of the taillike region and the tail-field increase. Finally, in the fourth section we review a theory [*Petschek and Kennel*, 1966; *Kennel*, 1969] for the inner edge of the electron plasma sheet based on the depletion of the plasma sheet by precipitation to the atmosphere as convection carries the plasma into the dipolar region of the earth's field. As originally posed [*Kennel*, 1969], this calculation suffered from the defect that the end of the dipolar region (or the beginning of the taillike region) was not specified. This difficulty is also alleviated by use of the Siscoe-Cummings procedure.

The models mentioned above are by no means mutually self-consistent nor is each model in itself complete and rigorously self-consistent. Furthermore, we have not explicitly included any of the dynamics undoubtedly occurring during growth phase, arguing that the relatively slow time development of the growth phase makes quantitative examination of the variations predicted by equilibrium considerations a reasonable first step. Our results may be regarded as most reliable if it is imagined that the growth phase proceeds arbitrarily slowly through a succession of near-equilibrium steady states. Our estimates of the changes in magnetosphere configuration based on this assumption are presented in the fifth section. The sixth section concludes with speculative remarks on substorms and magnetic storms.

Our calculations of the changes in magnetospheric structure during the substorm growth phase are at best crude but simple scaling relations by which frontside magnetospheric-configuration changes can be related to changes in the tail structure. We emphasize, therefore, not that the calculations do yield reasonable numerical agreement with the observed growth phase tail changes but that the observed tail changes logically follow from the shrinkage of the dayside magnetopause and the enhancement of internal convection.

FLARING-TAIL MODEL

In this section we review the flaring-tail model of *Tverskoy* [1968] and *Spreiter and Alksne* [1969]. The simplest model assumes the geomagnetic tail to be a bifurcated cylinder of radius $r = R_T(x)$, where x is the distance from the center of the earth along the axis of the cylinder, which is aligned with the solar wind. Henceforth we will use (r, x) coordinates appropriate to this cylindrical symmetry. A thin neutral sheet separates the northern and southern lobes, which have magnetic flux directed in the solar $(-x)$ and antisolar $(+x)$ directions, respectively. *Dungey* [1965] has estimated the length of the geomagnetic tail to be 1000 R_E; this estimate implies that for distances $x \ll 1000\ R_E$ the loss of magnetic flux from the lobes of the tail due to flux penetration across the tail magnetopause can probably be neglected. Henceforth we assume that the flux in the near-earth portion of the tail is constant with x.

To introduce notation and to motivate the necessity for a flaring tail, we briefly consider a nonflaring tail, with $dR_T/dx = 0$ so that the tail magnetopause has a zero angle of attack to the solar wind. Hence $B_T^2/8\pi|_{r=R_T} = P_0$, where P_0 is the static pressure in the magnetosheath. If the plasma density in the lobes of the tail is small, the magnetic field B_T must be nearly a vacuum field, whereupon B_T is uniform and is equal to $2F_T/\pi R_T^2$, where F_T is the flux in one lobe. Such a model has four consequences that are not borne out by observation. First, $B_T = (8\pi P_0)^{1/2} \approx 6.5\ \gamma$, whereas much larger tail fields are typically observed in the region $x = 20$–$40\ R_E$. Furthermore, the total plasma sheet pressure should also equal P_0. By contrast the particle energy density of the plasma sheet is always roughly 60% of the flow energy density [*Hones*, 1970] during steady solar-wind conditions. This finding immediately indicates that the tail is flaring [*Hones*, 1970]. Second, since F_T is almost constant, B_T should decrease by perhaps only 10% in the 100-R_E region downstream, whereas B_T has a strong x dependence in this region [*Mihalov et al.*, 1968; *Behannon*, 1968, 1970]. The findings are again consistent with a flaring tail. Finally, if F_T increases with time, as in the growth phase of magnetospheric substorms, R_T should increase, and B_T should remain constant. On the contrary, B_T increases by as much as 50% during the growth phase [*Camidge and Rostoker*, 1970; *Fairfield and Ness*, 1970; *Russell et al.*, 1971; *Aubry and McPherron*, 1971]. In fact, we will argue that near the earth R_T decreases during growth phase and that a nonflaring-tail solution only applies beyond 150 R_E downstream.

The above contradictions force consideration of a flaring tail, with $dR_T/dx > 0$. The assumption of constant tail flux is equivalent to neglecting the magnetic-field component normal to the tail magnetopause in the flaring region. Hence the radial B_r and axial B_x tail-field components must approximately satisfy the tangency condition for **B** at $r = R_T(x)$, $\epsilon B_r/B_x|_{r=R_T(x)} = \tan \alpha(x) = dR_T/dx$, where $\epsilon = \pm 1$ in the southern and northern lobes of the tail, respectively, and α is the angle of attack to the solar wind. If we assume weak flaring, $dR_T/dx \ll 1$, then B_r/B_x is small at the tail magnetopause, a fact that suggests that to first approximation we may neglect B_r throughout the lobes. Therefore a reasonable approximation is that

$$B_x = B_T = \epsilon 2F_T/\pi R_T^2(x) \qquad (1)$$

for near-vacuum field conditions. The condition of normal stress balance at the tail magnetopause is

$$\rho u^2 \sin^2 \alpha(x) + P_0 = B_x^2/8\pi|_{r=R_T(x)} \qquad (2)$$

Combining (1) and (2), with the assumption that $\sin \alpha \approx \tan \alpha \approx dR_T/dx \ll 1$, leads to

$$dR_T/dx = 1/M[(R_*/R_T)^4 - 1]^{1/2} \qquad (3)$$

which has the quadrature solution

$$\int_{R_0/R_*}^{R_T(x)/R_*} \frac{dr}{(r^{-4} - 1)^{1/2}} = \frac{x - x_0}{MR_*} \qquad (4)$$

In (3) and (4), $M^2 = \rho u^2/P_0$ is the sonic Mach number squared of the solar wind, where ρu^2 is the dynamic pressure, $R_* = (F_T^2/2\pi^2 P_0)^{1/4}$ is the asymptotic radius of the tail at the end of the flaring region ($dR_T/dx \to 0$), and $R_0 = R_T(x_0)$ is the initial radius of the tail at the downstream position x_0 where this tail solution is first valid. Flaring ceases at a finite distance x_* downstream, since the integral (5) below is finite:

$$\frac{x_* - x_0}{MR_*} = \int_{R_0/R_*}^{1} \frac{dr}{(r^{-4} - 1)^{1/2}} \simeq [0.6 - \tfrac{1}{3}(R_0/R_*)^3] \qquad (5)$$

Equation 5 is estimated in the appendix. For typical solar-wind values $P_0 = 1.7 \times 10^{-10}$ dynes/cm^2, $M \simeq 9$, and $R_* \simeq 15\ R_E(F_T)^{1/2}$, where F_T is units of 10^{16} Mx. For $F_T = 4 \times 10^{16}$ Mx, $R_* = 30\ R_E$, so that $x_* \simeq 140\ R_E$. Since this value is much less than the reconnection length of the tail, the assumption of constant total flux seems justified in the flaring region. Beyond x_* we may attach a nonflaring-tail solution of the appropriate length.

In the region $x_0 \ll x \ll x_*$, where most tail-field observations have been made, $r^{-4} \gg 1$, and thus a convenient approximate solution is

$$\frac{R_T(x)}{R_0} = \left(1 + \frac{x - x_0}{L}\right)^{1/3} \qquad (6)$$

$$B_T(x) = \frac{2F_T}{\pi R_0^2}\left(1 + \frac{x - x_0}{L}\right)^{-2/3} = (8\pi P_0)^{1/2}\left(\frac{R_*}{R_0}\right)^2\left(1 + \frac{x - x_0}{L}\right)^{-2/3} \qquad (7)$$

where L is the flaring-tail scale length, $L = MR_0^3/3\ R_*^2$. For constant P_0 and ρu^2, the above solutions are parametrized by the tail flux F_T and the initial tail radius and location, R_0 and x_0, respectively, or equivalently, R_*, R_0, and x_0. R_* can be estimated from the solar-wind pressure and the magnetic flux in the polar caps. R_0 and x_0 are more difficult to estimate. The aerodynamic solutions for flow around the magnetosphere of nose radius D, but with no tail magnetic structure, asymptotically approach a radius 1.6 D downstream [*Spreiter et al.*, 1966]. Hence a reasonable approximation is to take $R_0 = 1.6\ D$. The numerical factor 1.6 is probably variable, but the proportionality scaling $R_0 \propto D$ should yield a reasonably accurate estimate of the relative change in R_0 with respect to changes in D. From quiet-time tail magnetic observations [*Behannon*, 1968; *Mihalov et al.*, 1968] we expect $x_0 \simeq 10\ R_E$, although during disturbed conditions, when taillike fields are observed much closer to earth, x_0 may decrease to $<10\ R_E$. *Spreiter and Alksne* [1969] have shown that reasonable choices of M, R_0, R_*, and x_0 bracket the observed variation of B_T with x. Typical parameters are $M \simeq 9$, $R_0 = 16\ R_E$, $R_* = 30\ R_E$, $L = 14\ R_E$, and $x_0 = 10\ R_E$.

STRESS BALANCE FOR A FLARING TAIL

Our over-all goal is to evaluate the changes in tail magnetic structure predicted by the flaring-tail model that might occur during the substorm growth phase. Assuming that the solar-wind conditions remain constant, from observation we can estimate the changes in F_T and consequently in R_* and the changes in D and consequently in R_0. However, the initial tail

distance x_0 presents a difficulty, which we attempt to resolve by modifying for a flaring tail a procedure used by *Siscoe and Cummings* [1969] for estimating the effective distance x_T to the tail current sheet.

In a flaring tail the solar wind exerts a stress at the magnetopause that has one component perpendicular to the neutral-sheet plane and an x-directed component down the tail. The normal stress is balanced by magnetic pressure in the lobes and plasma pressure in the plasma sheet. *Siscoe and Cummings* [1969] have argued that, for the tail not to be continuously accelerated to hydromagnetic velocities, any x-directed stress on the tail must be statically balanced with the force of attraction between the earth's dipole and the fringing-tail magnetic field at the earth. The effective distance to the tail current sheet x_T adjusts until these two forces balance. In this section we estimate x_T for the flaring-tail model, still assuming that the plasma sheet remains thin at distances of the order of 10 R_E behind the earth. Since the Siscoe-Cummings calculation, which we use below, is not rigorously applicable to flaring tail, we can at best obtain a crude estimate of the distance x_T to the tail current system by the non-self-consistent combination of the Siscoe-Cummings and flaring-tail models; however, we hope that at least the scaling relations so obtained mirror some of the basic physics.

The x component of the solar-wind stress on a flaring tail is

$$S_x = (\rho u^2 \sin^2 \alpha + P_0) \sin \alpha = \frac{B_T^2(x)}{8\pi} \sin \alpha \simeq \frac{B_T^2(x)}{8\pi} \frac{dR_T}{dx} \quad (8)$$

and the net force is

$$f_x = 2\pi \int_{x_T}^{x_*} dx R_T(x) \frac{B_T^2}{8\pi} \frac{dR_T}{dx} = \frac{F_T^2}{\pi^2} \cdot \int_{R_0}^{R_*} \frac{R_T dR_T}{R_T^4} = \pi P_0 (R_*^2 - R_0^2) \frac{R_*^2}{R_0^2} \quad (9)$$

In (9) we have approximated x_T by x_0 so that the Siscoe-Cummings-tail and the flaring-tail models start at the same downstream distance. Since $R_0^2 \ll R_*^2$, we have roughly $f_x = F_T^2/2\pi^2 R_0^2$; hence f_x is relatively insensitive to the approximation $x_0 \simeq x_T$. The solar-wind force primarily depends on the flux in the tail and on its initial radius. To f_x should be added the force due to any tangential Maxwell stresses, which, since F_T is approximately constant in the flaring region, should be smaller than f_x.

One must balance f_x by the force of attraction to the dipole, given by the inner product of the earth's dipole moment $\mathbf{\mu}$ and the gradient of the tail-fringing field at the earth. The fringing magnetic field $b_T(x)$ along the midnight meridian at the geomagnetic equator, from a nonflaring cylindrical tail with a thin neutral sheet, is [*Siscoe*, 1966; *Siscoe and Cummings*, 1969]

$$b_T(x) = \frac{2j_T}{c} \left\{ \ln \left[\frac{(1 + d^2)^{1/2} + 1}{(1 + d^2)^{1/2} - 1} \right] - \frac{2}{(1 + d^2)^{1/2}} \right\} \quad (10)$$

where j_T is the tail current per unit length, and $d = (x_T - x)/(R_T) > 0$. Equation 10 should be valid for distances $x_T - x$ larger than the plasma sheet thickness. From (10)

$$\frac{db_T}{dx} = \frac{B_T}{\pi R_T d(1 + d^2)^{3/2}} \quad (11)$$

We will use the nonflaring estimates (10) and (11) as a rough approximation for the flaring tail. For B_T we substitute $B_T(x_T)$, the magnetic field at the entrance region to the flaring tail, and for R_T we substitute R_0, arguing that the nearest currents make the largest contribution to the fringing field. This argument undoubtedly overestimates the force of attraction to the dipole and the effective distance of the current sheet. The resulting approximate force balance is

$$\frac{\mu B_T(x_T)}{\pi x_T [1 + (x_T^2/R_0^2)]^{3/2}} = \frac{2\mu F_T}{\pi^2 R_0^2 x_T [1 + (x_T^2/R_0^2)]^{3/2}} = \frac{F_T^2}{2\pi^2 R_0^2} \quad (12)$$

which yields, as a solution for x_T,

$$x_T [1 + (x_T^2/R_0^2)]^{3/2} = \frac{10.3}{[F_T/(5 \times 10^{16})]} R_E \quad (13)$$

For $R_0 = 16\ R_E$ ($D = 10\ R_E$) and $F_T \simeq 4 \times 10^{16}$, $x_T \simeq 9\ R_E$, in reasonable agreement with observation.

INNER EDGE OF ELECTRON PLASMA SHEET

The magnetospheric configuration is also characterized by the location and structure of the

inner edge of the electron plasma sheet [*Vasyliunas*, 1968]. The inner edge has been observed to move earthward during or just prior to substorm expansion [*Vasyliunas*, 1968], this motion thus indicating that its location depends on the structure and dynamics of the tail. In this section we present a model of the inner edge first suggested by *Petschek and Kennel* [1966] in which the inner edge is primarily controlled by the effective distance to the tail current sheet.

When a convection electric field is present, plasma will flow toward the dipolar region of the geomagnetic field from the plasma sheet. The distance to which plasma can penetrate the dipole is limited by two effects, precipitation loss, and for sufficiently energetic particles, magnetic gradient and curvature drifts. In this section we consider only electron precipitation loss. Particle loss rates are limited by the size of the atmospheric loss cone, even when the pitch-angle diffusion coefficient is large. The minimum precipitation lifetime is $T_m = 2T_B/\alpha_0^2 \equiv 2T_BM$, where T_B is the particle's quarter bounce time, α_0 is the loss cone angle, and M is the mirror ratio [*Kennel*, 1969]. In a flowing plasma precipitation can produce a steep gradient in the particle distribution when the minimum lifetime is comparable with flow scale times to cross typical gradient lengths. In the geomagnetic tail particle loss is negligible; only when the flow penetrates the dipole is loss significant. Owing to the rapid spatial variation of the mirror ratio in the dipole region, a sharp inner edge is formed to the electron plasma sheet, where the flow time and minimum lifetime are first comparable [*Kennel*, 1969; V. M. Vasyliunas, unpublished manuscript referred to in *Kennel* [1969], 1969; *Wolf*, 1970].

A schematic calculation of strong-diffusion flow into a dipole is found in *Kennel* [1969]. However, in this calculation the distance to the end of the dipolar and beginning of the 'taillike' region was not specified. Here we will use the estimate of x_T in the third section to resolve this uncertainty. For simplicity, we assume that the magnetic field is essentially dipolar in the midnight meridian out to x_T. Since tail perturbations increase the mirror ratio and minimum lifetime, the flow will actually penetrate somewhat further than indicated here until it reaches a true dipolar region.

Using the techniques and assumptions of *Kennel* [1969], we find that the density $n(x)$ of hot electrons of plasma sheet origin has the profile

$$n(x) = n(x_T)\left(\frac{x_T}{x}\right)^4 \cdot \exp\left\{-\frac{3}{22}\frac{x_T}{\tilde{x}}\left[\left(\frac{x_T}{x}\right)^{22/3} - 1\right]\right\} \quad (14)$$

where $\tilde{x} = (cE/B)\, T_m|_{x=x_T}$. The electric field E is assumed constant and uniform up to the loss region; the electron gas is assumed adiabatic with an effective ratio of specific heats $\gamma = 5/3$ that is due to strong pitch-angle scattering. Under this assumption the electron temperature $T_e(x)$ obeys the scaling law $T_e(x) = T_e(x_T)(x_T/x)^{8/3}$, and the omnidirectional (and precipitation) flux $J = \frac{1}{4}n(T_e/m)^{1/2}$ scales as

$$J(x) = J(x_T)\left(\frac{x_T}{x}\right)^{16/3} \cdot \exp\left\{-\frac{3}{22}\left(\frac{x_T}{\tilde{x}}\right)\left[\left(\frac{x_T}{x}\right)^{22/3} - 1\right]\right\} \quad (15)$$

By differentiating (14) and (15) we find that the maximum hot-electron density occurs at $x_N = x_T(x_T/4\tilde{x})^{3/22}$ and that the maximum flux occurs at $x_J = x_T[(3/16)(x_T/\tilde{x})]^{3/22}$. The inner edge of the electron plasma sheet is the region $x < x_J$. Note that x_N and x_J are weakly dependent on the convection electric field, varying as $E^{-3/22}$, but strongly dependent on x_T.

TIME-DEPENDENT GEOMAGNETIC TAIL

The following things of relevance to tail dynamics appear to occur during the growth phase: the nose radius of the magnetopause decreases, magnetic flux is added to the tail, and a convection electric field is slowly established. The calculations of tail structure above are clearly inadequate for detailed absolute comparisons with observations. However, even though the various models are not mutually self-consistent, they do provide scaling relations through which the relative changes in the dayside magnetospheric structure during growth phase can be semiquantitatively related to relative tail changes during the growth phase. In this section we estimate the relative increase in the tail magnetic field, the magnitude of that portion of the field depressions at the ATS orbit due to increases in the tail-fringing field, and the earth-

ward motion at the inner edge of the plasma sheet from the known magnitudes of the dayside changes.

Since the Alfvén speed in the lobes of the tail is very large, the magnetic field will adjust very rapidly to changes in boundary conditions. Thus we can assume that, in evolving on the slow time scale of the substorm growth phase, at least the near tail passes through a succession of near-equilibrium states. From observation [*Aubry et al.*, 1970] the magnetopause nose radius D may decrease by $\Delta D/D \simeq -20\%$, and the tail flux F_T may increase by $\Delta F_T/F_T \simeq 10\%$ during the growth phase. If the initial tail radius R_0 scales as D, then R_0 should decrease as $\Delta R_0/R_0 = \Delta D/D \simeq -0.2$; since the asymptotic tail radius $R_* \propto F_T^{1/2}$, R_* increases during the growth phase. Therefore, the tail-flaring angle should increase, a fact implying that the tail intercepts more solar-wind dynamic pressure. Thus tail-field increases, enhanced solar-wind x-component stresses, and a decrease of the current sheet inner edge x_T should accompany frontside growth phase changes.

For slow or quasi-adiabatic configurational changes we can simply vary the tail solutions (7) to obtain the relative change in the near tail-field strength

$$\frac{\Delta B_T}{B_T} = \frac{\Delta F_T}{F_T}\left[1 - \frac{2}{3}\frac{x - x_0}{L + x - x_0}\right] - 2\frac{\Delta R_0}{R_0}\left[\frac{L}{L + x - x_0}\right] + \frac{2}{3}\frac{\Delta x_0/x_0}{[(L + x)/x_0] - 1} \quad (16)$$

where we have allowed the initial tail distance x_0 to vary. We do not have a self-consistent theory to determine x_0 and hence Δx_0. However, since the region of taillike field should move closer to the earth during the substorm growth phase, x_0 should decrease, and a plausible estimate assumes that $\Delta x_0/x_0 \approx \Delta x_T/x_T$, where x_T is determined by the Siscoe-Cummings procedure. Varying (13), we find

$$\frac{\Delta x_T}{x_T} = \frac{3\left(\frac{x_T}{R_0}\right)^2 \frac{\Delta R_0}{R_0} - \frac{\Delta F_T}{F_T}\left[1 + (x_T^2/R_0^2)\right]}{1 + (4x_T^2/R_0^2)} \quad (17)$$

which leads to $\Delta x_T/x_T \simeq -10$–$20\%$ for typical variations in $\Delta R_0/R_0$ and $\Delta F_T/F_T$. A somewhat more accurate computation is presented in Figure 1, where x_T is plotted as a function of total tail

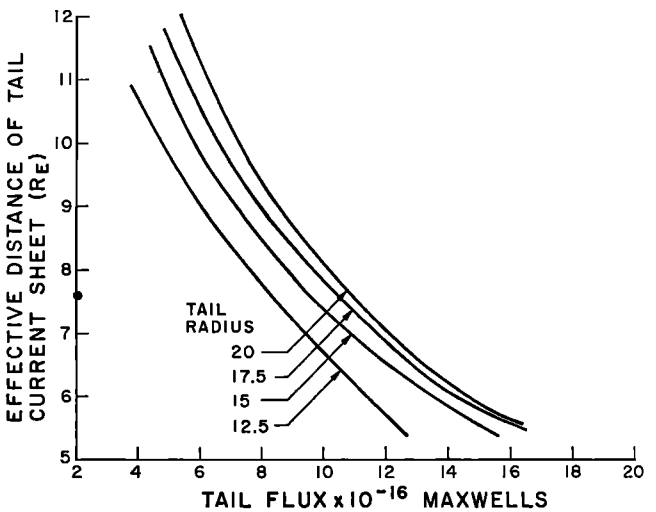

Fig. 1. Dependence of current sheet distance on tail radius and flux. Here we have reformulated the results of *Siscoe and Cummings* [1969] to allow for decreases in initial tail radius R_0 and simultaneous increases in tail flux F_T, here treated as the sum of the fluxes in both lobes. During a typical substorm growth phase F_T might increase by 10%, and R_0 might decrease by 20%.

flux (i.e., the sum of the fluxes in both lobes), with entrance radius R_0 as a parameter. Before the substorm growth phase F_T might be 8×10^{16} Mx, and $R_0 \simeq 15$–$17.5\ R_E$, at which point $x_T \simeq 9\ R_E$; at the end of the growth phase, F_T could increase to 9×10^{16} Mx, and R_0 could shrink to 12.5–15 R_E, at which point x_T decreases to 7.5–8 R_E. We now may estimate $\Delta B_T/B_T$ from (16). $\Delta F_T/F_T$ is typically 10%, and thus the increase in B_T from this source alone is only 3–10%, depending on $x - x_0$. Similarly, the decrease in B_T from $\Delta x_0/x_0$ is again only a few per cent. The dominant contribution to B_T stems from $\Delta R_0/R_0$, which produces 20–40% tail-field enhancements for downstream distances of 40 R_E or less. Therefore, the large increases in B_T observed during the substorm growth phase [*Camidge and Rostoker*, 1970; *Fairfield and Ness*, 1970; *Russell et al.*, 1971; *Aubry and McPherron*, 1971] cannot be explained semiquantitatively unless the nose of the magnetosphere shrinks. Other possibly observable effects during the growth phase include a decrease in the scale length L, a small increase in the asymptotic tail radius R_*, and a small increase to the end of the flaring region x_*.

The midnight meridian equatorial value of the tail-fringing field, at 6.6 R_E, which opposes the dipole field, is plotted in Figure 2 as a function of total tail flux, with R_0 as a parameter. If the flux increased but R_0 remained constant, the large depressions observed at geostationary orbit during growth phase [*Cummings et al.*, 1968; *Coleman and McPherron*, 1970] could not be due to the tail-fringing field. On the other hand, if the total tail flux increases from 8 to 9×10^{16} Mx and if R_0 decreases from 16 to 12.5 R_E, the perturbation field could increase from 13 to 34 γ. This possibility suggests that at least a portion of the time-dependent changes in magnetic configuration at geostationary orbit during the substorm growth phase may be due to changes in the tail-field configuration.

With regard to the motion of the inner edge of the plasma sheet, we note that electric-field increases during the growth phase cannot be responsible for the earthward motion of the inner edge of the plasma sheet [*Vasyliunas*, 1968] during the growth phase. Since the minimum lifetime scales as the magnetic mirror ratio, the earthward motion of the depressed field region associated with the plasma sheet

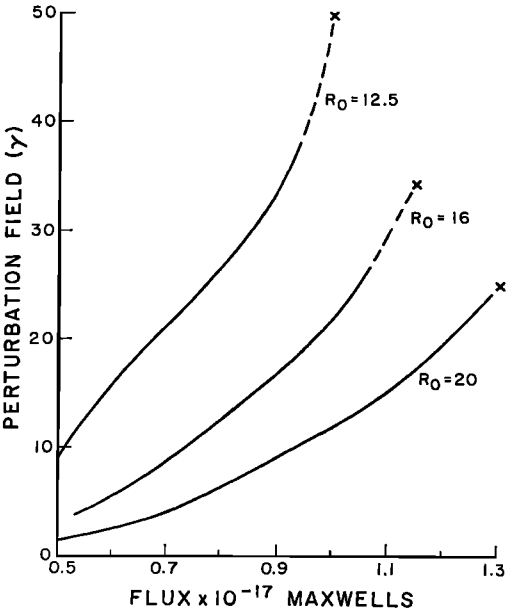

Fig. 2. Magnetic perturbations at geostationary orbit and dependence of ATS perturbation field on tail radius and flux. Here, by using (10), we have plotted the equatorial magnetic perturbations at local midnight in the geostationary orbit due to tail-field fringing as a function of R_0 and F_T. This perturbation subtracts from the dipole field to produce a depressed field during growth phase. The dotted lines indicate where the thin plasma sheet assumption contained in (10) may fail.

and tail-fringing field moves the region of long lifetime and the transition to dipolar field, where the inner edge is expected, closer to earth. Thus, as stated previously [*Kennel*, 1969], the motion of the inner edge of the electron plasma sheet is determined by gross changes in the magnetic configuration in the near-tail region.

Discussion

We have employed crude magnetospheric models, which are essentially scaling relations, to estimate the geomagnetic-tail configurational changes produced by the decrease in magnetopause nose radius and concomitant tail-flux increase observed during the growth phase. The semiquantitative agreement with tail observations may not be very significant by itself. What is significant, however, is that the tail configurational changes are logically consistent with the frontside magnetopause response to in-

creased field-cutting and enhanced internal convection. It appears, therefore, that such configurational changes should accompany any change in the convection rate. We review below a speculative picture of the substorm growth phase and comment briefly on magnetic storms.

The substorm growth phase commences with a southward shift in the solar-wind magnetic-field direction and enhanced field-cutting at the nose of the magnetosphere. Owing to ionospheric line-tying, flux is not initially returned to the dayside magnetopause at the rate at which it is peeled away by field-cutting [*Coroniti and Kennel*, 1971; *Tamao*, 1972]. This imbalance has two consequences. First, the dayside magnetopause must shrink by 1 or 2 R_E before the field-cutting and flux-return rates equalize. Such an equilibrium is approached roughly 20–60 min after the onset of enhanced field-cutting. The internal magnetospheric convection pattern is established on the same time scale. Second, since there is a finite interval of time during which the nose field-cutting rate exceeds the flux-return rate, a finite increment of flux is added to the geomagnetic tail. The shrinkage of the nose of the magnetosphere implies that the near tail also will be compressed. The addition of flux to the tail implies that, if no substorm intervened before the newly reconnected field lines traveled some 150 R_E to the end of the flaring region x_*, the asymptotic radius of the tail R_* would increase. Both effects increase the tail-flaring angle, and consequently large increases in tail field are expected. Increased flaring raises the downstream-directed stress exerted by the solar wind on the tail. For the tail to remain in quasi-static force balance the attractive force between the tail currents and the earth's dipole must increase. The tail currents move closer to earth, and their fringing-field increases. Similarly, the sharp inner edge to the plasma sheet electron distribution should move earthward, since the increase in tail magnetic field moves the transition to a dipolar field earthward, where the small mirror ratio ensures that electrons can be precipitated rapidly. Thus the nightside auroral oval should move equatorward [*Feldstein*, 1970; *Hirasawa and Nagata*, 1971].

During geomagnetic storms the magnetosphere should be even more strongly distorted. The much larger field-cutting rates expected suggest that the tail flux, rather than increasing by 10–20%, may in fact double. This possibility, together with the accompanying shrinkage of the nose of the magnetosphere, due to both field-cutting and increased solar-wind dynamic pressure, implies a large increase in tail flaring and magnetic field. The increased solar-wind flaring stress implies that the whole tail structure must move earthward, an implication that in turn implies that the inner edge of the electron plasma sheet must also move earthward. Since electron heat flux from the plasma sheet maintains the nightside auroral-oval ionosphere, auroral activity should move considerably equatorward during storms.

APPENDIX: CALCULATION OF INTEGRALS

The integral (5) may be rewritten as

$$\int_{R_0/R_{x*}}^{1} \frac{r^2\,dr}{(1-r^4)^{1/2}} \simeq \int_0^1 \frac{r^2\,dr}{(1-r^4)^{1/2}} - \int_0^{R_0/R_*} r^2\,dr \qquad \text{(A1)}$$

where we have used the approximation $(R_0/R_*)^4 \ll 1$. The substitution $r^4 = t$ reduces (A1) to

$$\frac{1}{4}\int_0^1 t^{-1/4}(1-t)^{-1/2}\,dt - \frac{1}{3}\left(\frac{R_0}{R_*}\right)^3 = \frac{\Gamma\left(\frac{3}{4}\right)\Gamma\left(\frac{1}{2}\right)}{\Gamma\left(\frac{5}{4}\right)} - \frac{1}{3}\left(\frac{R_0}{R_*}\right)^3 = 0.6 - \frac{1}{3}\left(\frac{R_0}{R_*}\right)^3 \qquad \text{(A2)}$$

where the form of (A2) identifies the integral as a complete β function $B(\frac{3}{4}, \frac{1}{2})$ and Γ denotes the usual gamma function.

The total magnetic energy W stored in the flaring-tail region may also be estimated:

$$W = \int_{x_0}^{x_*} \frac{B_T^2}{8\pi}\pi R_T^2\,dx = \frac{F_T^2}{2\pi^2}\int_{x_T}^{x_*}\frac{dx}{R_T^2(x)} \qquad \text{(A3)}$$

From (3) we find $dx = MdR_T/[(R_*/R_T)^4 - 1]^{1/2}$, and in consequence (A3) reduces to

$$\frac{F_T^2}{22\pi^2}\frac{M}{R_*}\int_{R_0/R_*}^{1}\frac{dr}{(1-r^4)^{1/2}} = M\pi P_0 R_*^3 \cdot\left[\int_0^1\frac{dr}{(1-r^4)^{1/2}} - \frac{R_0}{R}\right] \quad \text{(A4)}$$

The integral in (A4) is just $\frac{1}{4}B(\frac{1}{4},\frac{1}{2})$; consequently

$$W = M\pi P_0 R_*^3[1.3 - (R_0/R_*)] \quad \text{(A5)}$$

We note that the energy in the tail scales as $F_T^{3/2}P_0^{-1/4}(\rho u^2)^{1/2}$. For $R_* = 30\ R_E$, $P_0 = 1.7 \times 10^{-10}$, and $M = 9$, $W \simeq 2.5 \times 10^{22}$ ergs. A substorm dissipates roughly 10% of this energy.

Acknowledgments. It is a pleasure to acknowledge many informative conversations with M. P. Aubry and R. L. McPherron. R. W. Fredricks indicated the method of solution of the integrals in the appendix. W. I. Axford has been a constant source of encouragement. C. F. Kennel acknowledges the partial support of the Alfred P. Sloan Foundation, the University of Colorado, and the National Center for Atmospheric Research.

This research was contractually supported at UCLA by the Office of Naval Research, grant N00014-69-A-0200-4023; the National Science Foundation, grant GP-22817; the Atomic Energy Commission, contract AT(04-3)-34, project 157; and the National Aeronautics and Space Administration, contracts NGR-05-007-190 and NGR-05-007-116.

* * *

The Editor thanks G. Atkinson and V. M. Vasyliunas for their assistance in evaluating this paper.

REFERENCES

Akasofu, S.-I., Midday auroras and magnetospheric substorms, *J. Geophys. Res., 77,* 244, 1972.

Aubry, M. P., and R. L. McPherron, Magnetotail changes in relation to the solar-wind magnetic field and magnetospheric substorms, *J. Geophys. Res., 76,* 4381, 1971.

Aubry, M. P., C. T. Russell, and M. G. Kivelson, On inward motion of the magnetopause preceding a substorm, *J. Geophys. Res., 75,* 7018, 1970.

Behannon, K. W., Mapping of the earth's bow shock and magnetic tail by Explorer 33, *J. Geophys. Res., 73,* 907, 1968.

Behannon, K. W., Geometry of the geomagnetic tail, *J. Geophys. Res., 75,* 743, 1970.

Camidge, F. P., and G. Rostoker, Magnetic-field perturbations in the magnetotail associated with polar magnetic substorms, *Can. J. Phys., 48,* 2002, 1970.

Coleman, P. J., and R. L. McPherron, Fluctuations in the distant geomagnetic field during substorms, ATS 1, 171, in *Particles and Fields in the Magnetosphere,* edited by B. M. McCormac, D. Reidel, Dordrecht, Netherlands, 1970.

Coroniti, F. V., and C. F. Kennel, Magnetospheric substorms, paper presented at the European Physical Society Symposium on Cosmic Plasma Physics, Eur. Phys. Soc., Frascati, Italy, 1971.

Cummings, W. D., J. N. Barfield, and P. J. Coleman, Magnetospheric substorms observed at the synchronous orbit, *J. Geophys. Res., 73,* 6687, 1968.

Dungey, J. W., The length of the magnetospheric tail, *J. Geophys. Res., 70,* 1753, 1965.

Fairfield, D. H., Average and unusual locations of the earth's magnetopause and bow shock, *J. Geophys. Res., 76,* 6700, 1971.

Fairfield, D. H., and N. F. Ness, Configuration of the geomagnetic tail during substorms, *J. Geophys. Res., 75,* 7032, 1970.

Feldstein, Y.-I., Auroras and associated phenomena, paper presented at the International Symposium on Solar Terrestrial Physics, Leningrad, 1970.

Hirasawa, T., and T. Nagata, Space-time variation of aurora and associated phenomena, paper presented at IAGA-IAMAP Symposium on Morphology and Physics of Magnetospheric Substorms, IUGG Gen. Assem., Moscow, 1971.

Hones, E. W., Jr., Magnetotail plasma and magnetospheric substorms, in *Particles and Fields in the Magnetosphere,* edited by B. M. McCormac, p. 24, D. Reidel, Dordrecht, Netherlands, 1970.

Kennel, C. F., Consequences of a magnetospheric plasma, *Rev. Geophys. Space Phys., 7,* 379, 1969.

Meng, C.-I., Variation of the magnetopause position with substorm activity, *J. Geophys. Res., 75,* 3252, 1970.

Mihalov, J. D., D. S. Colburn, R. G. Currie, and C. P. Sonett, Configuration and reconnection of the geomagnetic tail, *J. Geophys. Res., 73,* 943, 1968.

Petschek, H. E., and C. F. Kennel, Tail flow, auroral precipitation, and ring currents, *Eos Trans. AGU, 47,* 137, 1966.

Russell, C. T., R. L. McPherron, and P. J. Coleman, Magnetic-field variations in the near geomagnetic tail associated with weak substorm activity, *J. Geophys. Res., 76,* 1923, 1971.

Siscoe, G. L., A unified treatment of magnetospheric dynamics, *Planet. Space Sci., 14,* 947, 1966.

Siscoe, G. L., and W. E. Cummings, On the cause of geomagnetic bays, *Planet. Space Sci., 17,* 1795, 1969.

Spreiter, J. R., and A. Y. Alksne, Effect of neutral sheet currents on the shape and magnetic field of the magnetosphere tail, *Planet. Space Sci., 17,* 233, 1969.

Spreiter, J. R., A. L. Summers, and A. Y. Alksne, Hydromagnetic flow around the magnetosphere, *Planet. Space Sci., 14,* 223, 1966.

Tamao, T., Unsteady magnetic-field annihilation between the magnetosphere and the solar wind, submitted to *J. Geophys. Res.*, 1972.

Tverskoy, B. A., *Dynamics of the Earth's Radiation Belts*, Physical-Mathematical Literature, Science Publishing House, Moscow, 1968.

Vasyliunas, V. M., A survey of low-energy electrons in the evening sector of the magnetosphere with Ogo 1 and Ogo 3, *J. Geophys. Res.*, *73*, 2839, 1968.

Wolf, R. A., Effects of ionospheric conductivity on convective flow of plasma in the magnetosphere, *J. Geophys. Res.*, *75*, 4677, 1970.

(Received November 5, 1971;
accepted March 15, 1972.)